SAND2008-1358C

Proceedings of PVP2008
2008 ASME Pressure Vessels and Piping Division Conference
27-31 July 2008, Chicago, IL
PVP2008-61269

EFFECT OF CHEMISTRY VARIATIONS OF WROUGHT N06022 PLATES ON THE REPASSIVATION POTENTIAL IN 1 M NaCl AT 90°C

Kevin G. Mon
Areva FS
1180 Town Center Dr.
Las Vegas, NV 89144, USA

Raul B. Rebak
GE Global Research
1 Research Circle
Schenectady, NY 12309, USA

ABSTRACT

ASTM standard B 575 provides the requirements for the chemical composition of Nickel-Chromium-Molybdenum (Ni-Cr-Mo) alloys such as Alloy 22 (N06022). The composition of each element is given in a range (e.g., the lowest content of Mo is specified as 12.5 weight percent and the highest as 14.5 weight percent. It is important to determine the dependence of Alloy 22 electrochemical behavior on the composition of the alloying elements as they vary from the lowest to the highest end of the ranges specified in ASTM B 575 standard. Seven heats of Alloy 22 plate were melted and processed. The plates were tested in the mill annealed (MA) and solution heat treated (SHT) condition. Cyclic potentiodynamic polarization tests were performed in 1 M NaCl solution at 90°C. Results show no influence of Alloy 22 chemistry variations or heat treating on the measured repassivation potential.

Keywords: N06022, Heat Composition Variability, Heat Treating, Repassivation Potential, ASTM G 61

INTRODUCTION

The composition of engineering alloys such as Alloy 22 (N06022) and 686 (N06686) is given by ASTM standards (e.g., ASTM B 575). [1] When the alloys are commercially produced their chemical composition may vary slightly from heat to heat while still within the boundaries of the ASTM B 575 standard specification. In general, for the commercial alloys the composition of the alloying elements is in the middle to lowest range of the standard [2].

The fabrication history of the original plates tested here is given in more detail elsewhere. [2-4] Basically, seven different heats (A through G) of wrought plates were fabricated (Table 1). The chemical composition of the plates generally varied from lean (Heat A) to rich (Heat G). Heat D also contained a larger amount of residuals such as Co, Mn, Al, Cu, V and Si. Heat G contained all the elements in the ASTM B 575 standard at their maximum values. All the base metal plates were prepared using commercial equipment and normal practices [3]. These plates were mill-annealed at 2050°F or 1120°C using standard mill practices [3]. The microstructure and mechanical properties of the seven MA plates were reported to meet ASTM and ASME specifications [2-3]. In previous works, the general corrosion behavior of similar plates was reported [4-5]. For the previous study two MA plates were also welded using gas tungsten arc welding (GTAW) using Alloy 686 filler wire. The corrosion rate was measured using immersion tests for the as-welded (ASW) and welded plus solution heat treated (SHT) specimens in the ASTM G 28A solution [6]. The solution heat treating or annealing was performed in air at 2075°F for 1 h plus rapid cooling (water spraying). [2-3]. Little or no effect of chemistry variations of 49 welded plates (7 heats of base metal x 7 heats of weld wire) was reported [4-5]. The coupons for the immersion tests contained both the base metal of Alloy 22 and the weld metal of Alloy 686 [4-5].

The objective of the current study was to perform electrochemical tests (ASTM G 59 and G 61) [6] to determine the corrosion rate and the crevice repassivation potential of the seven different heats of the base metal (Alloy 22) both for the

non-annealed and annealed conditions [3]. Annealing was done in air for 1 hour at 2075°F (1135°C) plus rapid cooling using water spraying. The Alloy 686 weld seam was not electrochemically tested in the current study.

EXPERIMENTAL

Preparation of the Specimens

The test material was delivered to Lawrence Livermore National Laboratory in the form of 1-inch thick welded plates from Allegheny Ludlum Co. For the purpose of this paper there were two types of plate strips: (1) Mill annealed (MA) and (2) solution heat treated (SHT). That is, the SHT base metal of Alloy 22 suffered two heat treatments, first the mill annealing of the plate before welding (at 2050°F or 1120°C) [3] and then the second solution annealing to homogenize the weld seam at 2075°F for 1 hour [2-3]. Again, the electrochemical study of the weld seam is not part of this paper. Table 2 shows the identification of the plates with the seven different chemistries. The specimens for the electrochemical tests were fabricated at LTI Inc. (Hatfield, PA) from the 14 listed plates (Table 2). Ten specimens from each plate were fabricated but only one specimen for each plate was tested in 1 M NaCl solution at 90°C. The specimens were prism crevice assemblies (PCA). Figure 1 shows the specimen assembled for testing with two crevice formers at each side secured by a bolt. Figure 2 shows a generic drawing of the specimen with the dimensions and other fabrication specifications. The use of the PCA creviced specimen to determine the crevice repassivation potential has been discussed before. [7-8].

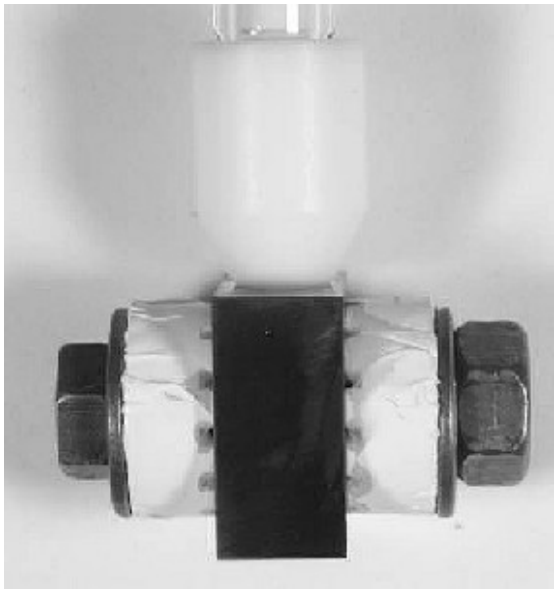

Figure 1. Assembled PCA specimen

Electrochemical Testing

Each specimen was wet ground with 600-grit SiC paper, and then ultrasonically cleaned in de-ionized water just before testing. Each specimen was then sandwiched by a pair of serrated ceramic crevice formers (ASTM G 78) with Teflon tape inserts [6], using a Ti Gr 2 bolt and nut to apply the desirable tightness or torque (70 in.lb or 7.9 N.m). Part of the Ti bolt was sleeved with Teflon tubing to prevent the bolt from making electrical contact with the test specimen. The specimen was then mounted in a specimen holder with electrical connection to run the polarization studies (Figure 1). The final exposed surface area for the specimen after the crevice assembling was 14.06 cm².

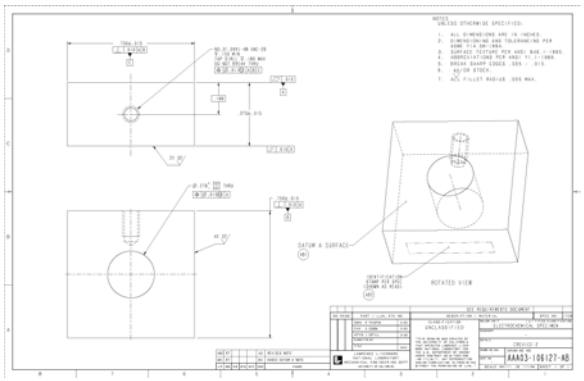

Figure 2. Drawing for the PCA Specimen

A three-electrode cell, with a capacity of one liter, was used for all the experiments. Generally, 800 mL of electrolyte solution was used in each test. A saturated silver/silver chloride (Ag/AgCl, pre-filled with 4 M KCl saturated with AgCl) reference electrode was used for measuring the potential of the working electrode. A Luggin probe solution bridge filled with the test solution was used to maintain an ionic conductive path between the working electrode and the reference electrode, while a cooling jacket was used to maintain the reference electrode at near room temperature. A platinum (Pt) sheet welded to a Pt wire was used as a counter electrode. The electrochemical cell was heated using a heating mantle. Nitrogen gas was bubbled through the test solution for deaeration. The gas exited the cell though a condenser and a liquid trap to prevent evaporation of the solution and the ingress of air into the test cell. The electrochemical polarization measurements were conducted through a commercial potentiostat that was integrated with a desktop computer and the companion software.

The electrochemical tests were performed in deaerated 1 M NaCl solution at 90°C. Each specimen was subjected to the same three-step test routine. The specimen was immersed in the deaerated brine at temperature and the free corrosion potential (E_{corr}) was monitored for 24 hours. The value of E_{corr} reported in Table 3 is the value of the potential at the end of the 24-hr

exposure (Step 1). After that, three consecutive polarization resistance tests (ASTM G 59) were carried out to estimate the general corrosion behavior of the specimens in the test solution (Step 2). In the last step a cyclic potentiodynamic polarization (CPP) test (ASTM G 61) was performed (Step 3).

For the polarization resistance a potential scan rate of 600 mV per hour (0.167 mV/s) was used. The potential was scanned from 20 mV below the instantaneous corrosion potential to 20 mV above the corrosion potential. This test lasts approximately 4 minutes. The corrosion rate was estimated from the polarization resistance tests using the following formulas given in ASTM standards G 59 and G 102 (6). The Polarization Resistance (R_p) is defined as the slope of the potential (E) vs. current density (i) at i = 0 (ASTM G 59) [6].

$$R_p = \left(\frac{\partial \Delta E}{\partial i} \right)_{i=0, dE/dt \to 0} \quad (2)$$

where $\Delta E = E - E_{corr}$. The corrosion current density, i_{corr}, is related to the polarization resistance R_p (in Ohm-cm²) by the Stern–Geary coefficient B (ASTM G 59)

$$i_{corr} = \frac{B}{R_p} \qquad B = \frac{b_a \cdot b_c}{2.303(b_a + b_c)} \quad (3)$$

where i_{corr} is in A/cm² and B is in V. b_a and b_c are the anodic and cathodic Tafel slopes in V

$$i_{corr} = \frac{1}{R_p} \times \frac{b_a \cdot b_c}{2.303(b_a + b_c)} \quad (4)$$

The corrosion rate can then be calculated using the Faraday equation (ASTM G 59)

$$CR(\mu m / yr) = k \frac{i_{corr}}{d} EW \quad (5)$$

Where k is a conversion factor (3.27 x 10^6 μm·g·A^{-1}·cm^{-1}·yr^{-1}), i_{corr} is the corrosion current density in μA/cm² (calculated from the measurements of R_p), EW is the equivalent weight, and d is the density of Alloy 22 (8.69 g/cm³). Assuming an equivalent dissolution of the major alloying elements as Ni^{2+}, Cr^{3+}, Mo^{6+}, Fe^{2+}, and W^{6+}, the EW for Alloy 22 is 23.28 (ASTM G 102) [6].

For the CPP tests the scan was started at 100 mV below the instantaneous corrosion potential and the scan was reversed when the current density reached 5 mA/cm². Both for the forward and reverse scans the potential scan rate was 0.167 mV/sec. From the CPP tests several parameters can be obtained. These are grouped into (1) Breakdown potentials (E20 and E200, which are the potentials in the forward scan that need to be reached to obtain current densities of 20 and 200 μA/cm² respectively) and (2) Repassivation potentials (ER10, ER1 and ERCO). ER10 and ER1 are the potentials in the reverse scan that need to be reached to obtain current densities of 10 and 1 μA/cm². ERCO is the potential at which the reverse scan crosses over (CO) the forward scan (Table 4).

RESULTS AND DISCUSSION

Corrosion Potential and Corrosion Rate

Table 3 shows the corrosion potential and corrosion rates after 24-hr immersion in the deaerated 1 M NaCl solution at 90°C. Both the corrosion potential and corrosion rates are for comparative purposes only for the testing conditions. The numbers in Table 3 do not represent the actual values for Alloy 22 after longer immersion times in the aerated 1 M NaCl electrolyte at the same temperature. Since Alloy 22 forms a passive film on the surface the corrosion potential is expected to increase and the corrosion rate decrease as time increases under aerated conditions [9].

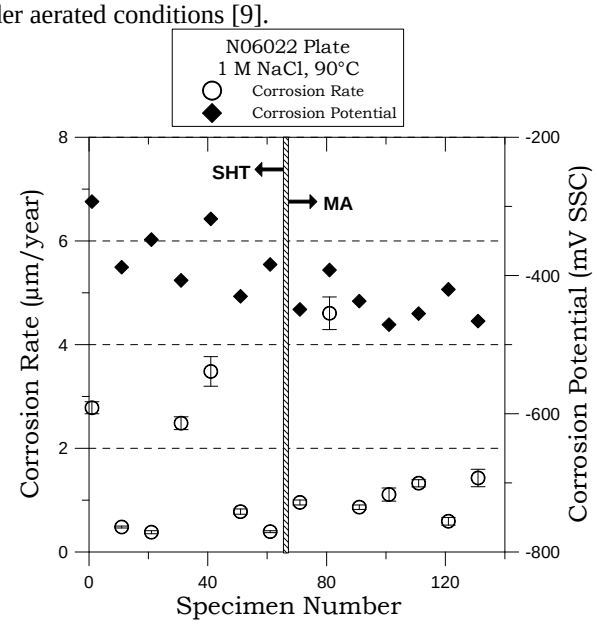

Figure 3. E_{corr} and Corrosion Rate after 24-hr immersion in deaerated 1 M NaCl, 90°C

Figure 3 shows in graphic form the data from Table 3. The corrosion rate (left Y-axis) is plotted for each specimen from HH001 to HH131. Seven specimens (HH001 to HH061 or Heats A to G) were solution heat treated (SHT) and seven specimens (HH071 to HH131 of Heats A to G) were mill annealed (MA). For each group of seven (Heats A to G) the pitting resistance equivalent (PRE) generally increased from A to G (Table 2). The lowest PRE was 66.7 for Heat A and the highest was 75 for Heat G. Figure 3 shows that the corrosion rate does not depend on the heat of the alloy or if the alloy has been SHT or not. For most cases the corrosion rate was in the order of 1 μm/year. There were a few corrosion rate outliers of about 4 times higher. However, this is common for Alloy 22 in the near neutral NaCl solutions. A high dispersion in the short term values of corrosion rate values has been reported before

[10]. Figure 3 also shows that the E_{corr} decreased as the heat number increased for each batch of specimens (SHT and MA). This could be only a coincidence. However, for the MA specimens the corrosion rate seemed to be higher when the corrosion potential was lower, which is expected [9].

Cyclic Potentiodynamic Polarization (CPP)

Figure 4 shows the CPP curves for SHT (HH011) and MA (HH081) Heat B material. The SHT material had a slightly lower breakdown and repassivation potentials than the MA material. This effect was reversed for the Heat D material where both characteristic potentials were lower for the MA material. Heat D is the heat with the highest amount of residuals such as Co, Al, Mn, V and Si (Table 1).

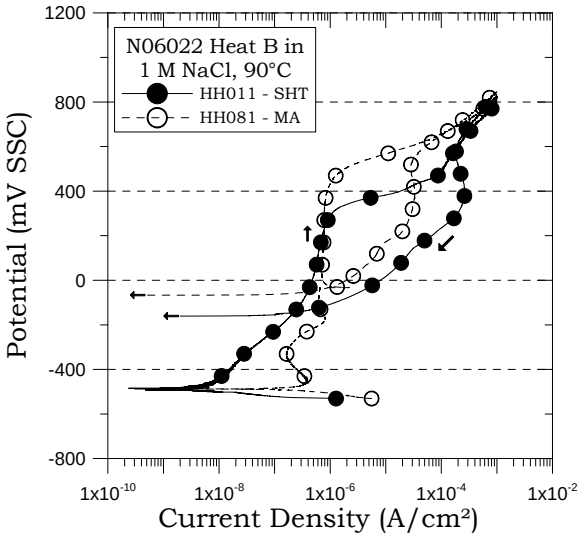

Figure 4. CPP for Heat B in 1 M NaCl at 90°C

Characteristic Potentials from the CPP

Instead of superimposing too many CPP curves, it is useful to extract characteristic potentials from the CPP plots and determine how they compare with each other. These characteristic potentials are breakdown potentials (E20 and E 200) and repassivation potentials (ER10, ER1 and ERCO). The characteristic potential values are listed in Table 4. Figure 6 shows the breakdown potential E20 for the seven SHT and MA Heats A to G. The E20 values vary by approximately 300 mV (from +350 mV to +650 mV SSC). As the heat number (and the PRE number in Table 2) increased the breakdown potential slightly increased. However the correlation was very poor. Also, Figure 6 shows that there is no significant effect of SHT vs. MA materials. In general the MA materials seemed to have slightly less dispersion. Table 5 shows that the archive measured values of E20 for commercial Alloy 22 heats was 285 ± 58 mV SSC [10, 11]. These archive values of E20 are below the lower band of potentials in Figure 6.

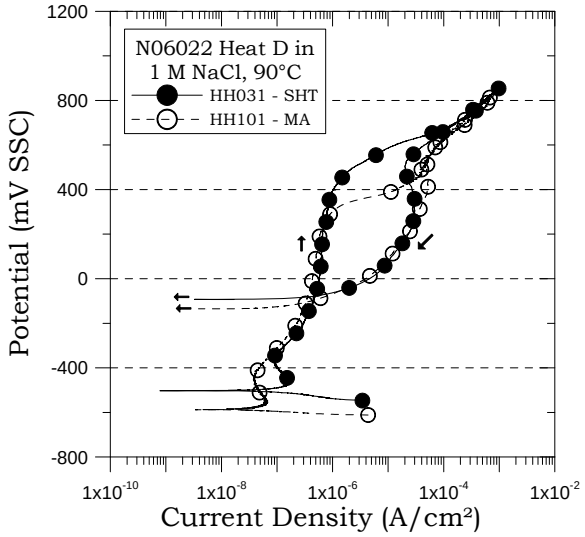

Figure 5. CPP for Heat D in 1 M NaCl at 90°C

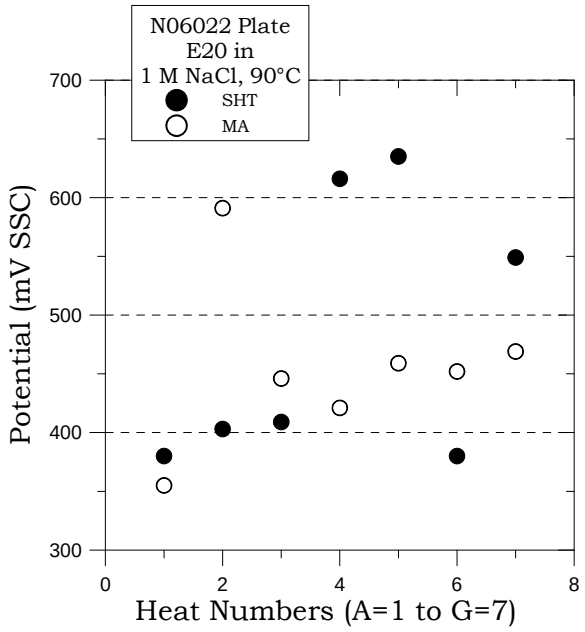

Figure 6. E20 for SHT and MA N06022 material

Figure 7 shows the values of the repassivation potential ERCO as a function of the PRE of the seven tested heats (Tables 2 and 4). Most of the values of ERCO both for the SHT and MA material were between -100 and -150 mV SSC. The average value of ERCO for the SHT specimens was -111 ± 60 mV SSC and the average value for the MA specimens was -116 ± 35 mV SSC. These two values are practically the same. In most of the heats the values of ERCO for SHT and MA

materials were close and there was no significant trend on the increase or decrease of the value of ERCO with the value of PRE (Figure 7). The average archive value for ERCO (Table 5) for commercial alloys is -69 ± 40 mV SSC for a PRE value of 70. The archive data fits (not shown) within the dispersion of the measured values shown in Figure 7.

The analysis of the data in Table 4 and Figure 7 shows that the repassivation potential value for Alloy 22 does not depend on the chemistry of the alloy within the specifications of ASTM B 575. Also, there is no apparent effect of SHT vs. MA on the value of the repassivation potential for wrought Alloy 22.

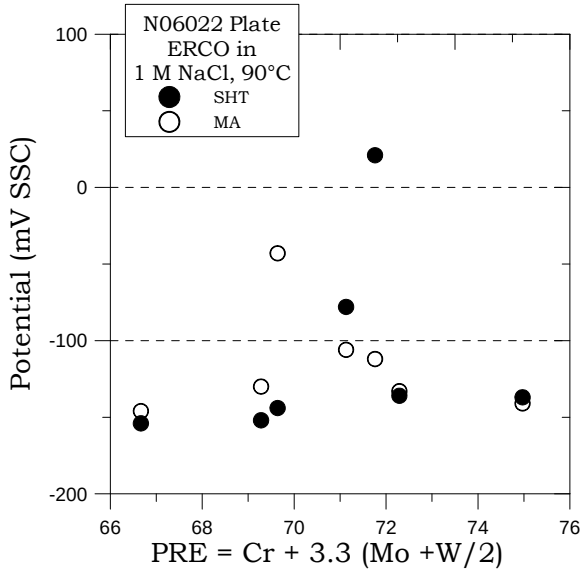

Figure 7. ERCO for SHT and MA N06022 material

Corroded Specimens

The 14 specimens shown in Table 2 showed crevice corrosion after the CPP tests. Crevice corrosion was typically a Type I (crystalline) event although some Type II (dull) has also been observed [12]. The attack typically occurred under the 24 crevicing sites or footprints of the PTFE coated ceramic crevice formers. Figures 8 and 9 show the post-CPP test appearance of the first and last specimen in Table 2. The 14 tested specimens also had transpassive attack on the non-creviced areas as a consequence of the high applied potentials of up to 800 mV SSC during the CPP test (Figures 4 and 5). The high applied potentials caused some of the specimens to have multiple colors including red, blue, green and yellow (Figures 8 and 9).

Figure 8. Specimen HH001 after the CPP test

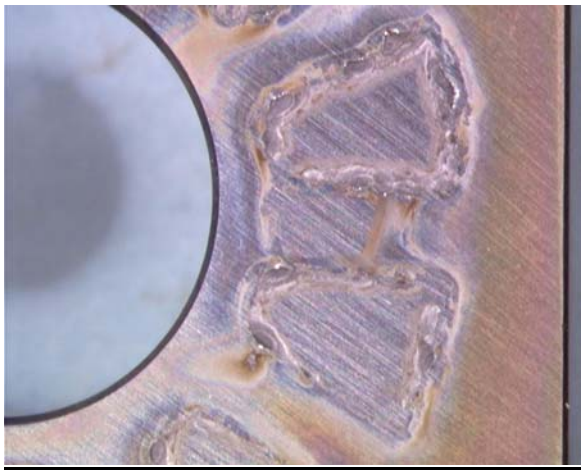

Figure 9. Specimen HH131 after the CPP test

CONCLUSIONS

- The repassivation potential of N06022 in 1 M NaCl at 90°C does not depend on its chemistry while within the specifications of ASTM B 575
- The repassivation potential for MA and SHT N06022 base plates was the same. The average value of ERCO for the SHT specimens was -111 ± 60 mV SSC and the average value for the MA specimens was -116 ± 35 mV SSC.
- In the range of the accepted chemistry of commercial N06022 materials the repassivation potential of one heat of material should represent the value of the repassivation potential of another heat of material.

ACKNOWLEDGMENTS

Phillip D. Hailey is acknowledged for performing the electrochemical tests in the laboratory. The fabrication of the specimens was supervised by John C. Estill. This work was partially performed under the auspices of the U. S. Department of Energy by the University of California Lawrence Livermore National Laboratory under contract W-7405-Eng-48. The work was supported by the Yucca Mountain Project, which is part of the DOE Office of Civilian Radioactive Waste Management (OCRWM).

REFERENCES

1. ASTM International, Annual Book of ASTM Standards, Volume 02.04 "Non-Ferrous Metals" Standard B-575 (West Conshohocken, PA: ASTM International, 2004).

2. Allegheny Technologies, Report on "Nickel-Based Alloy Weld Filler Material and Base Metal Composition Test Program', Report 004223-REV 000, March 2004 (Allegheny Technologies, 2004: Albany, OR).

3. J. F. Grubb and A. Nichols, "Base and Weld Metal Composition Effects on Weldment Mechanical Properties," Proceedings of the International High-Level Radioactive Waste Management Conference, Las Vegas, NV, 30 April to 4 May 2006, American Nuclear Society, pp. 813–820.

4. D. V. Fix and R. B. Rebak, "Effect of Chemistry Variations in Plate and Weld Filler Metal on the Corrosion Performance of Ni-Cr-Mo Alloys" - Paper 93417 in the Proceedings of PVP2006-ICPVT-11, Volume 7, p. 549, 2006 ASME Pressure Vessels and Piping Division Conference, July 23-27, 2006, Vancouver, BC, Canada

5. D. V. Fix and R. B. Rebak "Impact of Small Chemistry Variations in Plate and Weld Filler Metal on the Corrosion Performance of Ni-Cr-Mo Alloys," Journal of ASTM International, Vol. 3, No. 10, Paper ID JAI100401 (2006).

6. ASTM International, Annual Book of ASTM Standards, Volume 03.02, "Wear and Erosion; Metal Corrosion" (West Conshohocken, PA: ASTM International, 2004).

7. K. J. Evans and R. B. Rebak, "Measuring the Repassivation Potential of Alloy 22 Using the Potentiodynamic – Galvanostatic – Potentiostatic Method," Journal of ASTM International, Vol. 4, No. 9, Paper ID JAI101230 (2007)

8. K. J. Evans, A. Yilmaz, S. D. Day, L. L. Wong, J. C. Estill and R. B. Rebak, "Comparison of Electrochemical Methods to Determine Crevice Corrosion Repassivation Potential of Alloy 22 in Chloride Solutions," JOM, p. 56, January 2005

9. J. C. Estill, G. A. Hust, K. J. King, R. B. Rebak, TMS Letters, Volume 2, No.1, p.13-14 (2005).

10. S. D. Day, M. T. Whalen, K. J. King, G. A. Hust, L. L. Wong, J. C. Estill, and R. B. Rebak, *Corrosion*, 60, 804 (2004).

11. R. B. Rebak, R. A. Etien, S. R. Gordon, and G. O. Ilevbare, *Corrosion*, 62, 967 (2006).

12. R. B. Rebak, "Factors Affecting the Crevice Corrosion Susceptibility of Alloy 22," Paper 05610, Corrosion/2005, NACE International, April 03-07, 2005, Houston, TX (NACE International, Houston, TX)

Table 1. Approximate Average Chemical Composition of the Base N06022 Plates (Heats A-G)

	A	B	C	D	E	F	G
Ni	61.6	59.6	58.5	56.00	56.3	58.1	53.9
Cr	20.3	20.8	21.1	21.3	21.6	21.8	22.5
Mo	12.7	13.3	13.1	13.6	13.7	13.8	14.2
W	2.7	3.0	3.0	3.0	3.0	3.0	3.4
Fe	2.5	3.0	4.0	3.0	5.0	3.0	5.8
Co	0.15	ND	ND	2.23	ND	0.03	ND
Mn	0.02	0.02	0.01	0.4	0.04	0.02	0.03
Al	0.18	0.15	0.17	0.15	0.15	0.19	0.20
V	ND	ND	ND	0.25	0.01	0.01	0.01
Cu	0.01	0.01	ND	0.02	ND	0.01	ND
Si	0.03	0.03	0.03	0.07	0.04	0.05	0.05
C	0.004	0.004	0.006	0.005	0.01	0.014	0.007
S	0.0003	ND	ND	ND	ND	ND	ND
P	0.003	0.004	0.004	ND	0.006	0.005	0.006

ND = Not Detected

Table 2. Specimen Designation

Specimen	Heat	Plate	Condition	PRE
HH001	A	85R1	SHT	66.7
HH011	B	45R1	SHT	69.6
HH021	C	37R1	SHT	69.3
HH031	D	177R1	SHT	71.1
HH041	E	135R1	SHT	71.8
HH051	F	127R1	SHT	72.3
HH061	G	29R1	SHT	75.0
HH071	A	50R1	MA	66.7
HH081	B	44R1	MA	69.6
HH091	C	168R1	MA	69.3
HH101	D	176R1	MA	71.1
HH111	E	190R1	MA	71.8
HH121	F	72R1	MA	72.3
HH131	G	122R1	MA	75.0

PRE = Pitting Resistance Equivalent = Cr + 3.3 (Mo + W/2)
Where the symbols of the elements represent their weight percent (Table 1)
For an average commercial N06022 heat the value of PRE = 70

Table 3. 24-hr Corrosion Potential (mV SSC) and Corrosion Rates (µm/year)

Specimen	24-hr E_{corr} (mV SSC)	Average Corrosion Rate (µm/year)	SD Corrosion Rate
HH001	-293	2.782	0.117
HH011	-388	0.482	0.018
HH021	-348	0.382	0.029
HH031	-407	2.485	0.124
HH041	-318	3.483	0.285
HH051	-430	0.778	0.051
HH061	-384	0.393	0.020
HH071	-449	0.956	0.048
HH081	-392	4.605	0.315
HH091	-437	0.865	0.043
HH101	-471	1.109	0.126
HH111	-455	1.326	0.070
HH121	-420	0.593	0.074
HH131	-466	1.428	0.169

Table 4. Typical Potentials from the Cyclic Potentiodynamic Polarization Tests

Specimen	E20 (mV SSC)	E200 (mV SSC)	ER10 (mV SSC)	ER1 (mV SSC)	ERCO (mV SSC)
HH001	380	537	-4	-127	-154
HH011	403	606	17	-108	-144
HH021	409	638	-23	-126	-152
HH031	616	710	79	-63	-78
HH041	635	736	125	26	21
HH051	380	670	1	-111	-136
HH061	549	732	-23	-119	-137
HH071	355	488	-3	-117	-146
HH081	591	695	173	-30	-43
HH091	446	691	3	-110	-130
HH101	421	683	96	-68	-106
HH111	459	701	40	-83	-112
HH121	452	688	16	-99	-133
HH131	469	721	-3	-116	-141

Table 5. Archive data for Commercial N06022 in 1 M NaCl at 90°C [10,11]
All the specimens were non-welded MCA (lollipop)

Specimen	E20 (mV SSC)	E200 (mV SSC)	ER10 (mV SSC)	ER1 (mV SSC)	ERCO (mV SSC)
DEA3129	234	674	25	-51	-24
DEA3130	291	582	-14	-75	-67
JE3324	261	438	-38	-117	-126
JE3328	228	475	-33	-113	-109
DEA3262	384	634	28	-95	-42
DEA3263	311	605	17	-101	-45
Average	285	568	-3	-92	-69
Standard Dev.	58	92	30	25	40